A&A 396, 203–211 (2002)
DOI: 10.1051/0004-6361:20021424
© ESO 2002

Astronomy & Astrophysics

Starspots and active regions on the emission red dwarf star *LQ Hydrae*⋆

I. Yu. Alekseev and O. V. Kozlova

Crimean Astrophysical Observatory, P/O Nauchny, 98409 Crimea, Ukraine
Isaac Newton Institute of Chile, Crimean Branch, Ukraine

Received 19 October 2001 / Accepted 26 September 2002

Abstract. The quasi-simultaneous electrophotometric, polarimetric and spectroscopic observations of the single active spotted star *LQ Hya* are presented. The photometric variability of the star can be described completely by a zonal starspots model. Spotted regions occupy up to 23% of the total stellar surface. The temperature difference between the unspotted photosphere and starspots is about 800 K. Starspots are localized at the low and middle latitudes. We find for the first time broad-band linear polarization of the stellar light and its rotational modulation connected to the local magnetic region on the stellar surface. We suspect that there is a spacial connection between plages, magnetic regions and the mostly spotted stellar longitudes.

Key words. stars: activity – stars: chromospheres – stars: magnetic fields – starspots

1. Introduction

Spots are of ten percent on cool low luminosity dwarf stars. An axial rotation of a spotted star and slow variations of the starspot geometry cause so-called the BY Dra-type photometric variability. Stars of this type form a group consisting of more than 112 spotted red dwarf stars with spectral types from G0Ve to M6Ve (Alekseev 2000). The BY Dra-type photometric variability is expressed in brightness rotational modulation and slow variations of mean stellar brightness. The magnetic field of starspots causes the Zeeman polarization effect. It is detected in broad-band linear polarimetric observations (Piirola 1977; Huovelin et al. 1985, 1988, 1989; Alekseev 2000b). All BY Dra-type variables are chromospherically active and show emission lines in their spectra. One of the most typical lines for such stars is a hydrogen emission H_α.

LQ Hya (Gl 355 = HD 82558 = BD-10°2857) is a young dK0e single BY Dra-type variable star probably just arriving on the zero-age main sequence. Its age according to the lithium LiI6707.8 Å line observations is about 7.5×10^7 years (Fekel et al. 1986a). The photometric variability of *LQ Hya* was found by Eggen (1984) and Fekel et al. (1986a) in 1982. Later these observations were continued by Strassmeier & Hall (1988) and Boyd et al. (1990). Long-term series of photometric observations carried out by Jetsu (1993), Cutispoto (1991, 1993, 1996, 1998a,b), Cutispoto et al. (2001), Strassmeier et al. (1993, 1997) suggest the presence of the cycle of stellar activity like the solar one (Oláh et al. 2000). Strassmeier et al. (1993) and Alekseev & Gershberg (1996a) made a simulation of the *LQ Hya* starspots. Their results strongly depend on the input starspot geometry, for example, some high-latitude spots (Strassmeier et al. 1993) or low-latitude spotted belts (Alekseev & Gershberg 1996ab).

Fekel et al. (1986a,b) noted for the star very strong emissions in chromospheric CaII H and K lines, in the far ultraviolet, and the completely filled H_α line. Vilhu et al. (1991) found the variations of H_α emission with a time scale of about year, and fast (days) variability, not correlated with the stellar rotation. At the same time, Strassmeier et al. (1993) showed the presence of rotational modulation in the CaII and H_α chromospheric line parameters. These facts indicate that the H_α chromospheric emission may be formed as in the chromospheric network, so in active regions above starspots (Strassmeier et al. 1993).

The aim of the present study is to understand active regions on the *LQ Hya* surface. We have thus constructed starspots models for *LQ Hya* on the basis of the total set of published and original photometric observations. We also consider the connection between starspots, chromospheric activity and magnetic regions.

2. Observations and results

2.1. Photometry

The photometric observations used the 1.25 m telescope AZT-11 of the Crimean Astrophysical Observatory equipped with the *UBVRI* double image chopping photometer-polarimeter of Piirola (Piirola 1984, 1988; Kalmin 1995; Kalmin & Shakhovskoy 1995). All *LQ Hya* measures were obtained with respect to HD 82508 (G2III, $V = 7\overset{\mathrm{m}}{.}58$, $U - B = 0\overset{\mathrm{m}}{.}35$, $B - V = 0\overset{\mathrm{m}}{.}71$, $V - R = 0\overset{\mathrm{m}}{.}59$, $V - I = 1\overset{\mathrm{m}}{.}03$,

Send offprint requests to: I. Yu. Alekseev,
e-mail: ilya@crao.crimea.ua

⋆ Table 5 is only available in electronic form at
http://www.edpsciences.org

Article published by EDP Sciences and available at http://www.aanda.org or http://dx.doi.org/10.1051/0004-6361:20021424

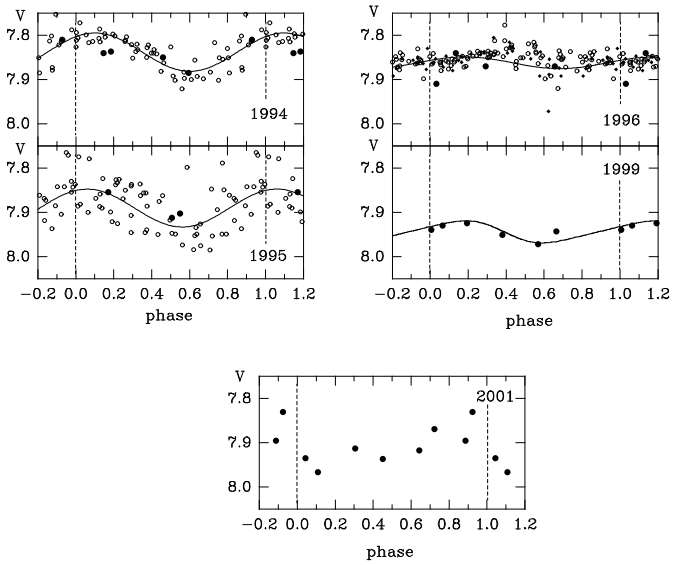

Fig. 1. Light curves of *LQ Hya* in the *V* band. Our data are denoted as points, the T7 Vienna University automatic telescope observations (Strassmeier et al. 1997) denoted as open circles, and the *APT Phoenix* observations denoted as diamonds.

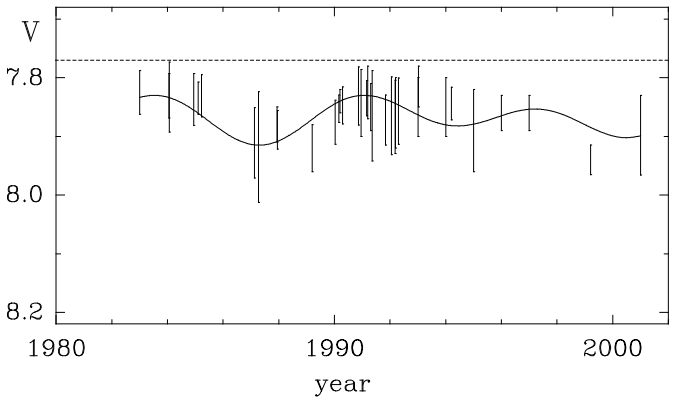

Fig. 2. Long-term light curve of *LQ Hya* in the *V* band. The vertical bars indicate the peak-to-peak amplitude of the light curves, and the solid line indicate the fit with two periods by Oláh et al. (2000).

Cutispoto 1991), hereafter $c1$; and HD 82477 (K2III, $V = 6\overset{\mathrm{m}}{.}13$, $U-B = 0\overset{\mathrm{m}}{.}49$, $B-V = 1\overset{\mathrm{m}}{.}18$, $V-R = 0\overset{\mathrm{m}}{.}89$, $V-I = 1\overset{\mathrm{m}}{.}52$, Cutispoto 1991) was used as a check star $c2$. All observations utilized Johnson *UBVRI* filters. The measurement of each star consists of four 10-s integrations averaged in each filter. A complete observation sequence consists of three $c1-\mathrm{var}-c2-c1$ sets averaged to obtain one data point. The observations were corrected for atmospheric extinction and transformed into the standard Johnson *UBVRI* system. The typical accuracy of the photometry of program stars is $0\overset{\mathrm{m}}{.}01$. The previous results of our *LQ Hya* photometric observations were published in (Alekseev 1998, 1999, 2001; Alekseev & Gershberg 1996a).

LQ Hya was observed regularly during 1994, 1999 and 2001. During 1995 and 1996 there were a few measurements only. Light curves of *LQ Hya* in the *V* band are shown in Fig. 1. The data were phased with a photometric period computed by Jetsu (1993):

$$\mathrm{JD} = 2\,445\,274.220 + 1.601135E. \qquad (1)$$

In 1994–1996 the star was observed by Strassmeier et al. (1997). Their data are also given in Fig. 1.

In 1995 and 1996 the rotational modulation amplitude ΔV decreased from $0\overset{\mathrm{m}}{.}08$ to $0\overset{\mathrm{m}}{.}02$ with the roughly constant mean brightness level. In 1994 and 1999 the light curves had a single-peaked shape approximated by a sine with amplitude $\Delta V = 0\overset{\mathrm{m}}{.}09$ and $0\overset{\mathrm{m}}{.}05$, respectively. The light curve in 2001 had an irregular shape with the rotational modulation amplitude $0\overset{\mathrm{m}}{.}14$. The mean stellar brightness varies slowly from year to year with a magnitude of about $0\overset{\mathrm{m}}{.}10$. The location of the light curve minimum remained stable during 1994–1999. The color variations agree with the *V* band modulation, showing the star is redder at light minimum. The results of our *LQ Hya* photometric observations are given in Table 1.

The long-term light curve of *LQ Hya* was built first by Jetsu (1993) and Strassmeier et al. (1993, 1997). We added our data and extended the total time coverage to the year 2001 (Fig. 2).

From Fig. 2, we can see that the rotational modulation amplitude ΔV varies from $0\overset{\mathrm{m}}{.}04$ in 1990 to $0\overset{\mathrm{m}}{.}19$ in 1987. At the same time, the mean brightness of the star changed relatively weakly. The amplitude of its variations is equal to about $0\overset{\mathrm{m}}{.}10$. Oláh et al. (2000) showed that the photometric behaviour of *LQ Hya* can be approximated with two periods of 11.4 and 6.75 years. Our observations agree very well with this result (Fig. 2). The star was in the brightest state in 1984 and 1991 with $V_{\mathrm{abs}} = 7\overset{\mathrm{m}}{.}77 \pm 0\overset{\mathrm{m}}{.}01$, which we assumed to be an unspotted magnitude. The corresponding absolute brightness is $M_V = 6\overset{\mathrm{m}}{.}40$.

We compared values of the stellar brightness in *UBRI* Johnson bands with the *V* band ones. The data by Cutispoto (1991, 1993, 1996, 1998a,b), Cutispoto et al. (2001) and Strassmeier et al. (1993, 1997) in *RI* bands were reduced from the Cousins system into the Johnson one using the dependences found by Bessel (1979). From this comparison we can see that the brightnesses in the *UBRI* bands depend linearly on *V* band magnitude. Such dependences are typical for *BY Dra* type variables. The corresponding linear regression coefficients are: $\mathrm{d}U/\mathrm{d}V = 1.29 \pm 0.15$, $\mathrm{d}B/\mathrm{d}V = 1.10 \pm 0.11$, $\mathrm{d}R/\mathrm{d}V = 0.74 \pm 0.01$ and $\mathrm{d}I/\mathrm{d}V = 0.67 \pm 0.01$. Taking into account these values and the maximum brightness value $V_{\mathrm{abs}} = 7\overset{\mathrm{m}}{.}77 \pm 0\overset{\mathrm{m}}{.}01$ we can obtain the color indices of the *LQ Hya* unspotted photosphere: $U-B = 0\overset{\mathrm{m}}{.}52 \pm 0\overset{\mathrm{m}}{.}m01$, $B-V = 0\overset{\mathrm{m}}{.}90 \pm 0\overset{\mathrm{m}}{.}01$, $V-R = 0\overset{\mathrm{m}}{.}76 \pm 0\overset{\mathrm{m}}{.}01$, $V-I = 1\overset{\mathrm{m}}{.}32 \pm 0\overset{\mathrm{m}}{.}01$. These color indices are redder than the typical values for a normal K0V star. Thus the absolute magnitude of the *LQ Hya* unspotted photosphere and its color indices correspond rather to a K2V star.

2.2. Polarimetry

The simultaneous photometric and linear polarimetric *UBVRI* observations were carried out in March 2001 on the 1.25 m telescope AZT – 11. The measurement of a comparison star or a check star consisted of eight 10-s integrations in each filter corresponding to the eight $\lambda/2$ polarizer positions. Each measurement of *LQ Hya* was carried out in four series.

Table 1. *UBVRI* photometric observations of *LQ Hya*.

epoch	number of nights	$< V >$	ΔV	$U-B$	$B-V$	$V-R$	$V-I$	phase
1994.3	5	7.84	0.09	0.59	0.88	0.78	1.33	0.60
1995-6	7	7.88	0.07	0.58	0.87	0.80	1.35	0.6
1999.2	6	7.94	0.05	0.59	0.88	0.82	1.38	0.57
2001.2	8	7.90	0.14	0.60	0.87	0.80	1.29	0.1

This technique allows us to obtain a typical accuracy on the P_x and P_y Stokes parameter measurements of about 0.02% in the U band and 0.01% in other bands and to confirm our photometric accuracy.

In Table 2 we list results of the *UBVRI* linear polarimetric observations of *LQ Hya*. For each passband we give the averaged Stokes parameters P_x and P_y with their deviations, the results of the standard χ^2 test (the reduced $\chi^2/(N-1)$ values with $N-1$ degrees of freedom), and the probability $F_{\rm var}$ that the Stokes parameters are variable. The $F_{\rm var}$ value should then provide an estimate of the significance of the observed variations. Also we give the average of the most significant polarization degree deviations from zero in each passband. These are values $P_{\rm s}$ of average polarization degree of 2σ greater than zero. This definition of $P_{\rm s}$ correctly determines the degree of linear polarization for stars with a large net P (Huovelin et al. 1988).

We can see from Table 2 that the star shows significant linear polarization and variations of the Stokes parameters in all passbands. The growth of the average polarization degree from I band to U is clearly seen. The largest amplitudes of the Stokes parameter variations are seen in the U band: 0.30% for P_x and 0.23% for P_y, respectively. In Fig. 3 the linear polarization degree and the position angle in U band are presented as a function of the photometric phase. One can see that the phase of the maximum polarization differs from the phase of the minimum brightness (i.e. maximum spot area) 0.25 of the rotation period. This difference depends on the spot size and is typical of magnetic spots (Huovelin & Saar 1991).

We can estimate a filling factor of the magnetic region using any assumption about the broad-band linear polarization origin. In this paper we shall consider the magnetic intensification effect only, because the contribution of the Thompson scattering is negligible, and Rayleigh scattering is probably a significant contributor in polarization only for stars with low gravity and extended atmospheres (not dwarfs) (Huovelin & Saar 1991). Saar & Huovelin (1993) showed that the maximum polarization degree is proportional to coefficient A which depends from the spotarea S as

$$A(S) = -2.128\times10^{-4} + 1.076S - 4.812S^2 + 9.058S^3 - 6.26S^4, \quad (2)$$

where S is given in percent. Saar & Huovelin (1993) computed expecting values of maximum polarization degrees in *UBVRI* bands for the range of 4000 K $< T_{\rm eff} <$ 6500 K and 3.0 $<$ log $g <$ 4.5. Using these data, we can estimate from $P_{\rm s}$ the value of the magnetic region filling factor. In our estimations we assume that the local magnetic field strength is about 2–3 kGs (as typical for K0V − K2V stars, Saar 1996).

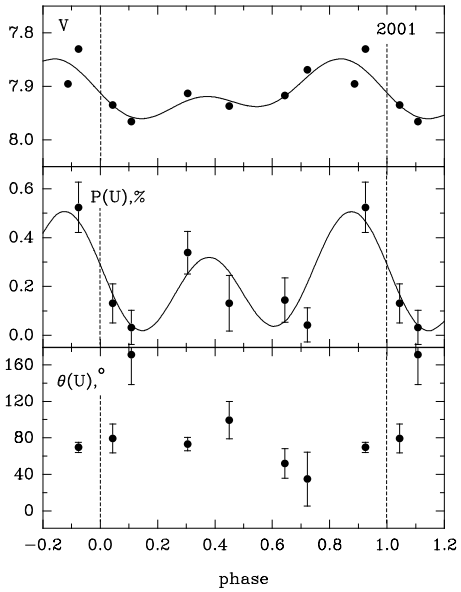

Fig. 3. Light curve of *LQ Hya* in the V band and polarization degree P and position angle θ in the U band as a function of photometric phase. The continuous lines are the weighted 2nd order Fourier fits. The beginning and the end of non-duplicated data marked by dashed lines.

In Fig. 4 the comparison of observed maximum polarization values $P_{\rm s}$ (points) in 2001 with the maximum possible polarization for magnetic intensification model (dashed line) in *UBVRI* bands are shown. One can see that in U and B bands the maximum observed polarization degree $P_{\rm s}$ corresponds to the maximum possible value, i.e. the magnetic region filling factor is about $S = 24\%$ of the total stellar surface. This value agrees with our estimations of starspot area in the same year (see below). In the *VRI* bands the observed $P_{\rm s}$ values are greater than the theoretical polarization ones. We can explain this result by an additional source of polarization, for example, a circumstellar disk remains (*LQ Hya* is a relatively young star having infrared excess).

2.3. Spectroscopy

The high resolution ($R = 20\,000$) spectroscopic observations of *LQ Hya* were carried out on 13 nights from December 1998 to March 2001 with the 2.6 m Shain telescope of the Crimean observatory, equipped with a Coudé spectrograph and a 1024 × 256 pixel CCD camera. All observations in the H_α wavelength

Table 2. Linear polarization of *LQ Hya* in 2001.

band	$< P_x >$	σ	$\chi^2/(N-1)$	$F_{\rm var}$	$< P_y >$	σ	$\chi^2/(N-1)$	$F_{\rm var}$	$< P >$	σ	$P_{\rm s}$
U	−0.150	0.156	3.63	99	0.157	0.203	3.56	99	0.246	0.225	0.284 ± 0.093
B	−0.036	0.061	2.90	95	−0.126	0.078	3.05	98	0.148	0.065	0.164 ± 0.022
V	−0.011	0.062	6.69	99	−0.091	0.074	5.37	99	0.132	0.072	0.116 ± 0.022
R	−0.026	0.026	2.42	92	−0.082	0.067	7.42	99	0.094	0.049	0.126 ± 0.011
I	0.005	0.031	1.36	60	−0.082	0.045	3.35	99	0.093	0.035	0.090 ± 0.014

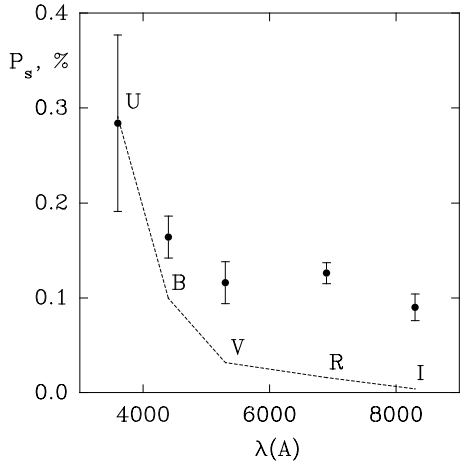

Fig. 4. Wavelength dependence of the polarization degree. Points show observational estimations of the maximum polarization degree $P_{\rm s}$, and the dashed curve shows the expected theoretical dependence in *UBVRI* bands.

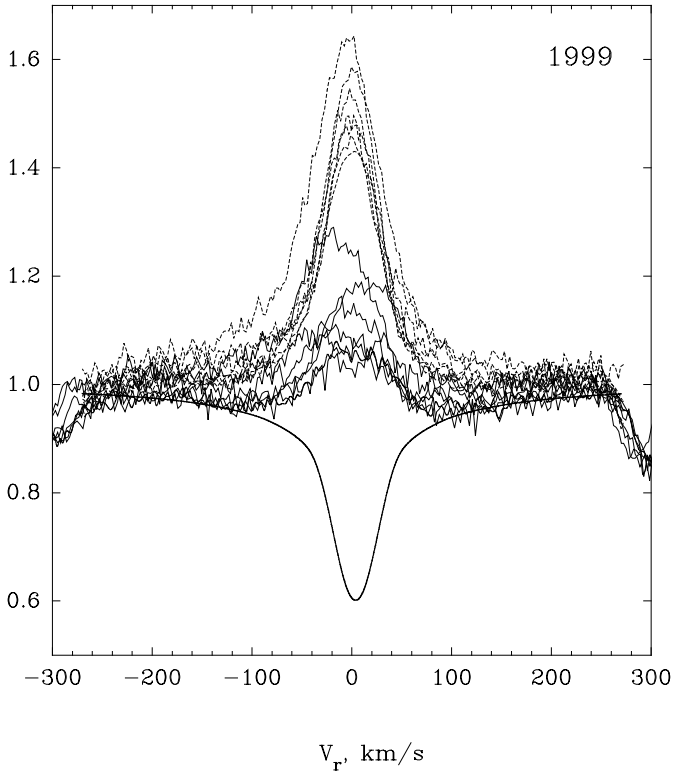

Fig. 5. a) H_α line profiles for *LQ Hya* in 1998–1999. The thin lines show the observed spectra, the thick lines show the synthetic spectra, and the dashed lines show the residual pure emission spectra.

region were made in the second order of the spectrograph with a resolution about 0.3 Å and a useful wavelength range of 60 Å. All integrations had an exposure of about 20–30 min and a typical signal–to–noise relation of about 70–130. The images were cleaned of cosmic particles and corrected by the flat field. The obtained spectra were reduced with the help of numerical code *SPE* by S. G. Sergeev. We used observations of a bright early-type fast rotating star for the atmospheric water correction.

All obtained spectra are presented in Figs. 5a, b (thin lines). They are superimposed on synthetic spectra (thick lines) calculated with the help of the *SYNTH* and *ROTATE* programs of Piskunov (1992), and the *VALD* database of atomic spectral-line parameters (Piskunov et al. 1995, 1999). The synthetic spectrum was computed with the following model: $T_{\rm eff}$ = 5000 K, log g = 4.0, $V \sin \iota$ = 25 km s^{-1}, $V_{\rm micro}$ = 0.5 km s^{-1}, $V_{\rm macro}$ = 1.5 km s^{-1}. The same model was adopted by Rice & Strassmeier (1998) for the Doppler Imaging. Residual pure emission spectra (dashed lines) are also shown in Fig. 5.

In all spectra one can clearly see the absorption H_α wings and the emission core with a central reversal at the rest wavelength. This central reversal is typical of active red dwarfs and formed by the optically thick chromosphere. All spectra show the H_α line asymmetry: one emission peak (most often "blue") is stronger than the other. The reasons for this asymmetry discussed by Strassmeier et al. (1993) are a weak chromospheric velocity field and a rotational modulation by bright plages. On the one hand, one can see that for some spectra (17.02.99, 24.01.01 and 17.03.01) the "red" peak appears stronger than the "blue" one indicating the bright plage presence. On the other hand, the width of emission line indicates gas motion on the line of sight with typical velocities up to 80 ÷ 100 km s^{-1}. Thus, these velocities are connected with large-scale motions of gas in chromosphere. Some spectra (9.12.99, 11.12.99) demonstrate blue asymmetry of the H_α emission profile. This asymmetry is seen as an extend emission wing reaching the value −150 km s^{-1}. Thus, we can see a combination of stellar plages moving in and out of view and local velocity fields.

In Table 3 we give the main characteristics of the H_α line: Julian Date HJD of the spectrum and the corresponding phase; ratios $F_{\rm max}/F_{\rm cont}$ of the peak emission flux to the continuum flux for real spectra and the same for the pure emission; the distance between the "blue" and the "red" peaks $\Delta\lambda_{\rm peak}$; the $F_{\rm red}/F_{\rm blue}$ ratio of the peak fluxes; the width of the pure emission profile $FWHM$ and the equivalent width of the pure emission value.

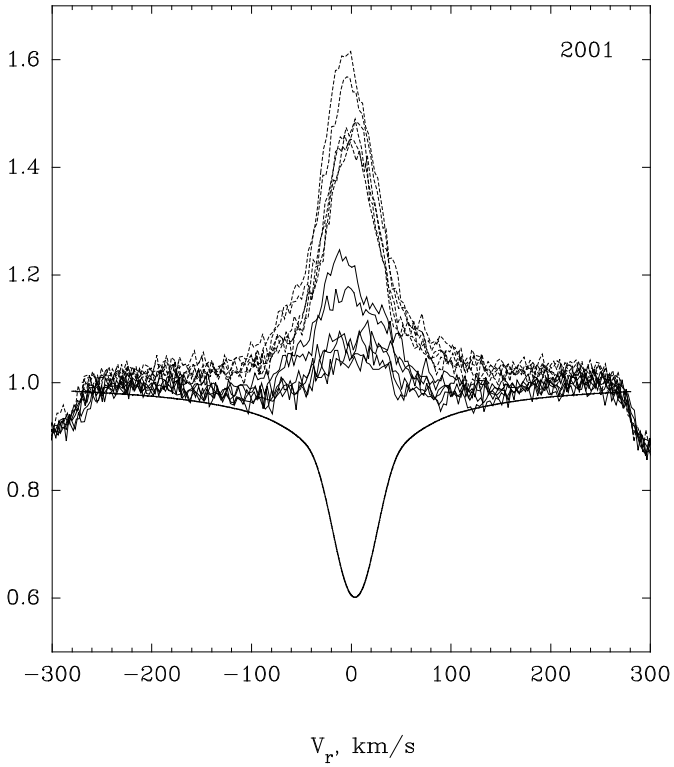

Fig. 5. b) H_α line profiles for *LQ Hya* in 2001 year.

We may roughly estimate physical parameters for the lower chromospheres of *LQ Hya* given by the model of Cram & Mullan (1979) assumptions. It is a model of an optically thick isothermal chromosphere. The optical depth of the isothermal chromosphere is

$$\ln \tau_{\rm chrom} = (\Delta\lambda_{\rm peak}/2\Delta\lambda_{\rm D})^2, \quad (3)$$

where $\Delta\lambda_{\rm D}$ is the Doppler width. For the typical chromospheric temperature $T_{\rm chrom}$ = 10 000 K this value is equal to about 0.28 Å. Thus, the chromospheric optical depth may vary in active regions from 6 to 200 depending on rotational phase. The electron density may be estimated by:

$$n_{\rm e} = 1.67 \times 10^{14} (F_{\rm max}/F_{\rm cont})(B(T_{\rm eff})/B(T_{\rm chrom}))\tau^{-1}_{\rm chrom}. \quad (4)$$

For the Table 3 data, $n_{\rm e}$ varies from 9.0×10^{10} to 3.0×10^{12} cm^{-3}. These values agree with those estimated by Strassmeier et al. (1993). It is important to note that if $n_{\rm e} \sim 6 \times 10^{11}$ cm^{-3} the replacement of the collisional line formation mechanism by the photoionization one must be done.

3. The starspots model simulations

To find the area and temperature of the spot region, we must know the brightness of the unspotted photosphere and the relations between the Δm values at different wavelengths which can be estimated from the observations. In our calculations we use the $V_{\rm abs}$ value and the coefficients dB/dV, dR/dV and dI/dV. We must also make some initial assumptions about the spotted region configurations.

Traditional algorithms lead to large near-pole circular spots on all red dwarfs of any spectral type. This conclusion contradicts the solar spots picture. On the other hand, Eaton et al. (1996) showed that the aggregate of many (5–40) low-latitude starspots can fit the photometric behaviour of any real spotted star.

Alekseev & Gershberg (1996a,b, 1997) showed that the spotted regions on cool stars can be represented by two spotted belts located symmetrically about the equator. These belts occupy regions with latitudes from $\pm\phi_0$ to $\pm(\phi_0 + \Delta\phi)$ and have a spot coverage that varies linearly with longitude from 1 at the minimum brightness phase to some value $f_{\rm min}$ at the maximum brightness phase, where $0 < f_{\rm min} < 1$. Such a zonal model can fit any light curve without the second humps. The model was applied to several spotted red dwarfs with the spectral classes from G2 to M4.5 and rotation velocities up to 25 km s^{-1} (Alekseev 2001; Alekseev & Gershberg 1997; Alekseev & Kozlova 2000, 2001) and these results were in qualitative agreement with the pattern of solar spots. It should be noted that our algorithm did not impose any restriction on definable spot latitudes with the exception of a natural limit $\phi_0 + \Delta\phi < 90°$, where it produces a polar spot. Thus the spot latitudes are the definable variables depending on the dB/dV, dR/dV and dI/dV coefficients (the value $\phi_0 + \Delta\phi/2$ increasing with the dB/dV growth and anticorrelating with dR/dV and dI/dV, Alekseev & Gershberg 1996b).

In our calculations we use two input variables. They are the brightness rotational modulation amplitude ΔV, and the difference between the maximum stellar brightness in every season and the brightness of the unspotted photosphere $\Delta V_{\rm max}$. The five input parameters of the spot modelling are following: the coefficients dB/dV, dR/dV and dI/dV, the inclination of the stellar rotation axis ι and the stellar photosphere temperature $T_{\rm phot}$. We calculate the radiation deficit at *BVRI* bands creates by starspots by Dorren (1987). The limb-darkening coefficients were taken from van Hamme (1993).

To estimate the inclination angle $\iota = 70°$, we use the values of the rotation velocity $V \sin\iota = 25 \pm 2$ km s^{-1}, the stellar radius $R = 0.79\ R_\odot$ and the photometric period $P_{\rm rot} = 1\overset{\rm d}{.}601136$ given by Jetsu (1993). The photospheric temperature $T_{\rm phot}$ = 5000 K was estimated by using the calibration of Johnson (1966) from the $(V - R)$ and $(V - I)$ color indices of the unspotted photosphere. Strassmeier et al. (1993) and Rice & Strassmeier (1998) obtain similar $T_{\rm phot}$ values from the spectral classification and the model of the photosphere. The starspots models for *LQ Hya* are given in the Table 4.

According to this table, the photometric behaviour of *LQ Hya* can be explained by a zonal model where the distance from the spotted belts to the stellar equator is from $\phi_0 = 24°$ to $\phi_0 = 34°$. The spotted belt width $\Delta\phi$ varies from 9° to 25°. Thus, the mean latitude of starspots is about 33–40°. The coverage parameter $f_{\rm min}$ varies from 0.00 to 0.67, which yields a total spotarea $S_{\rm max} + S_{\rm min}$ up to 22.5% of the total stellar surface. The ratio of the brightnesses of the spots and the quiet photosphere β_V varies from 0.31 to 0.37 corresponding to a temperature difference ΔT of about 800 K.

Table 3. Spectroscopic observations of *LQ Hya* in H_α region.

HJD	phase	F_{max}/F_{cont} original profile	F_{max}/F_{cont} pure emission	$\Delta\lambda_{peak}$ original profile	$FWHM$ original profile	F_{red}/F_{blue} original profile	EW Å
51163.6404	0.276	1.08	1.46	0.98	1.28	0.97	0.75
51199.5183	0.684	1.18	1.59	0.86	1.68	0.99	1.09
51227.3891	0.091	1.06	1.42	0.83	1.25	1.01	0.72
51244.3119	0.660	1.15	1.55	0.74	1.42	0.99	0.91
51522.5996	0.466	1.10	1.50	1.08	1.40	0.98	1.05
51524.5956	0.713	1.29	1.64	0.92	1.78	0.97	1.59
51525.5932	0.336	1.12	1.48	1.29	1.54	0.97	0.98
51934.3916	0.654	1.07	1.45	1.19	1.47	1.03	0.82
51935.3931	0.279	1.09	1.49	0.92	1.47	1.00	0.83
51951.3827	0.266	1.18	1.57	1.12	1.58	0.99	1.15
51982.3210	0.589	1.25	1.62	0.92	1.54	0.92	1.18
51983.3711	0.244	1.09	1.45	1.12	1.47	0.95	0.82
51986.3844	0.126	1.11	1.48	1.06	1.30	1.07	0.78

3.1. Comparison with other models

Our values of the total spot area demonstrate very good agreement with the starspot mapping results obtained by other methods such as light curve simulations (Strassmeier et al. 1993) and Doppler Imaging (Strassmeier et al. 1993; Saar et al. 1992, 1994; Rice & Strassmeier 1998; Donati 1999; Berdyugina et al. 2001).

The results of the light curve simulations (Strassmeier et al. 1993) and Doppler Imaging (Strassmeier et al. 1993; Saar et al. 1992, 1994; Rice & Strassmeier 1998; Donati 1999) give the ΔT values of about 500−600 K and up to 700 K. Results of Doppler Imaging by Berdyugina et al. (2001) and starspot temperature estimated by the spectral observations of the TiO molecular bands (Saar & Neff 1990) agree with our estimations very well.

For the latitudinal distribution of the spotted regions we see a good agreement with the results of Doppler Imaging showing the existence of medium-latitude and low-latitude starspots. But the same results show also near-polar spots, which are not shown by our calculations.

We considered the following starspots models: the zonal model, the model of three rectangular spots (Strassmeier et al. 1993), the model of a near – polar spot and the Doppler Imaging. For each model we constructed synthetic light curves in *BVRI* bands and obtained the difference between the maximum stellar brightness in every season and the unspotted photosphere brightness ΔV_{max}, the amplitude of rotational modulation ΔV, and the coefficients dB/dV, dR/dV, dI/dV. A comparison between these parameters with the observational ones is presented in Table 5 is only in electronic form at `http://www.edpsciences.org`.

The zonal model shows a good representation of observations for all epochs.

The model of three rectangular near-equatorial spots (Strassmeier et al. 1993) gives a good agreement with the observations in 1991 for ΔV_{max} and ΔV values, but for the coefficients dB/dV and dI/dV the agreement with observations is significantly worse.

For **the model of near-pole spot** we see a good agreement for ΔV_{max} and ΔV in all epochs excepting 1994.3 and 1999.2 when this agreement is slightly worse. In the epoch 1995.0 the ΔV_{max} and ΔV parameters fit the observations not well. For all epochs we do not see a good agreement with observations for the coefficients dB/dV, dR/dV and dI/dV.

The Doppler Imaging carried out by Berdyugina et al. (2001) gives for all epoches the coefficients dB/dV, dR/dV and dI/dV close to the ones calculated with the zonal model. The ΔV_{max} and ΔV parameters in the epoch 1994.0 are close to our results too. In the epoch 1994.3 the ΔV_{max} and ΔV parameters fitting is not very good, and in the epoch 1999.3 we do not see any agreement in these parameters.

The Doppler Imaging carried out by Strassmeier et al. (1993), Rice & Strassmeier (1998) and Donati (1999) do not give a satisfactory agreement with the observations both for ΔV_{max} and ΔV parameters and for dB/dV, dR/dV, dI/dV coefficients.

Thus, the zonal model fits the photometric behaviour of *LQ Hya* much the same as other starspots models. Doppler Imaging needs quasisimultaneous photometric observations to construct self-consistent starspots model.

4. The starspots – active regions connection

In previous papers (Alekseev & Kozlova 2000, 2001) we noted that the active regions (plages) for the chromospherically active binaries V 775 Her and VY Ari are concentrated near the most spotted longitude. We present in Figs. 6a, b the light curves of *LQ Hya* in 1999 and 2001 compared with the H_α line behaviour as a function of rotational phase.

In 1999 the light curve minimum corresponding to the most spotted longitude coincides with the maximum of the pure emission equivalent width EW, the width of the pure emission profile $FWHM$ and the relative pure emission intensity F_{max}/F_{cont}. This effect indicates the presence of the chromospherically active regions (plages) which concentrate at the most spotted regions.

Table 4. Starspots parameters of *LQ Hya*.

epoch	$\Delta V_{\max}$	ΔV	ϕ_0	$\Delta\phi$	$f_{\min}$	β_V	$S_{\max}$	$S_{\min}$	reference
1983.00	0.014	0.075	33	12	0.00	0.37	7.6	2.5	1
1984.05	0.020	0.076	32	12	0.00	0.36	7.8	2.6	2
1984.07	0.000	0.119	32	16	0.00	0.35	10.4	3.5	1
1984.95	0.020	0.088	31	13	0.00	0.36	8.6	2.9	3
1985.10	0.034	0.055	31	10	0.20	0.37	7.1	3.6	3
1985.23	0.022	0.072	32	12	0.03	0.37	7.7	2.8	3
1987.12	0.078	0.120	25	20	0.23	0.33	13.7	7.1	4
1987.27	0.053	0.189	24	25	0.03	0.31	16.1	5.8	4
1987.95	0.083	0.066	27	15	0.41	0.35	11.0	7.2	5
1989.20	0.110	0.080	25	18	0.45	0.34	13.4	9.1	6
1990.03	0.065	0.075	28	15	0.30	0.35	10.6	6.1	4
1990.16	0.056	0.047	30	11	0.39	0.37	8.3	5.3	4
1990.2	0.05	0.04	30	10	0.41	0.37	7.1	4.6	7
1990.29	0.042	0.063	31	12	0.22	0.37	8.6	4.4	4
1990.87	0.011	0.099	32	15	0.00	0.36	9.8	3.3	4
1990.96	0.012	0.114	31	16	0.00	0.35	10.5	3.5	4
1991.10	0.010	0.090	32	13	0.00	0.35	8.4	2.8	8
1991.15	0.010	0.060	34	9	0.00	0.37	6.1	2.0	8
1991.3	0.04	0.08	30	14	0.15	0.36	9.5	4.3	9
1991.36	0.014	0.154	29	21	0.00	0.34	13.5	4.5	4
1991.83	0.056	0.085	28	15	0.22	0.35	10.6	5.5	4
1992.05	0.029	0.133	28	19	0.00	0.34	12.0	4.0	4
1992.18	0.034	0.125	28	18	0.02	0.34	11.8	4.1	4, 10
1992.30	0.027	0.113	30	17	0.00	0.35	11.1	3.7	4
1993.0	0.03	0.10	30	16	0.03	0.35	10.2	3.7	11
1993.02	0.01	0.07	34	11	0.00	0.37	7.4	2.5	12
1994.0	0.01	0.12	31	17	0.00	0.35	10.9	3.6	11
1994.30	0.03	0.09	31	15	0.05	0.36	9.8	3.7	11, 13–16
1995.0	0.08	0.08	27	17	0.35	0.35	11.9	7.2	11
1996.0	0.08	0.02	30	10	0.72	0.37	8.2	7.0	11
1997.0	0.06	0.06	29	13	0.34	0.36	9.3	5.6	17
1999.2	0.15	0.05	24	17	0.67	0.33	13.7	11.2	this
2001.1	0.06	0.14	26	21	0.12	0.33	14.3	6.2	paper

1) Fekel et al. (1986a); 2) Eggen (1984); 3) Strassmeier & Hall (1988); 4) Jetsu (1993); 5) Cutispoto (1991); 6) Cutispoto (1993); 7) Cutispoto (1996); 8) Strassmeier et al. (1993); 9) Cutispoto (1998a); 10) Cutispoto (1998b); 11) Strassmeier et al. (1997); 12) Cutispoto et al. (2001); 13) Alekseev & Gershberg (1996a); 14) Alekseev (1998); 15) Alekseev (1999); 16) Alekseev (2001); 17) Strassmeier et al. (1999).

On the other hand, in 2001 such effect is absent. The variations of the H_α parameters do not correlate with the spot area and show the large scattering. This effect indicates the uniform distribution of plages.

In Fig. 7, we present the dependence of the pure H_α emission equivalent width on the stellar brightness and the dependence of the H_α luminosity on the total spotarea on *LQ Hya* constructed on the basis of our observations and literature data (Fekel et al. 1986a,b; Vilhu et al. 1991; Strassmeier et al. 1990, 1993; Montes et al. 1999; Thatcher & Robinson 1993).

The *V* band magnitudes in Fig. 7a were measured from the unspotted photosphere brightness. The strong photometric variability does not lead to considerable variation in the H_α pure emission equivalent width (the *EW* value varies from 0.47 to 1.59 Å). Figure 7b takes into account the variations of the continuum level in the 6563 Å wavelength region. It demonstrates the comparison of the chromospheric luminosity with the spot area. The methods of the $L_{\rm chr}$ estimation from the equivalent width *EW* value were described by Alekseev et al. (2001). Based on the absolute magnitudes of *LQ Hya* in the Johnson *R* band at the observed epoch M_R, we transformed the pure H_α emission equivalent width *EW* into absolute luminosity using the well-known calibration of the Johnson (1966) *R* band:

$$L(\mathrm{H}_\alpha) = 2.1 \times 10^{31-0.4M_R} EW \ \mathrm{erg/s}. \quad (5)$$

The total radiative losses from the stellar chromosphere $L_{\rm chr}$ can be estimated from the relation $L_{\rm chr} = L(\mathrm{H}_\alpha)/kl$ where k is the ratio of the H_α line flux to to the total Balmer flux and l is the ratio of the Balmer emission to the total radiation losses. According to Sundland et al. (1988), and Shakhovskaya (1974), H_α emits about 53% of the total chromospheric Balmer line emission. Further, the contribution of the Balmer lines to the total radiative losses from the chromosphere depends on the spectral type and ranges from 13% for the Sun to 77% for UV Cet (Pettersen 1987). The l value for *LQ Hya* is about 18%.

We can see from Fig. 7b, that the spotarea growth from 2 to 12% of the total surface corresponds to $L_{\rm chr}$ variations from 5.12×10^{29} to 1.57×10^{30} erg/s, which are not correlated with the spot area. The bolometric luminosity deficit caused by starspots varies from 1.02×10^{31} to 5.78×10^{31} erg/s. Thus, the

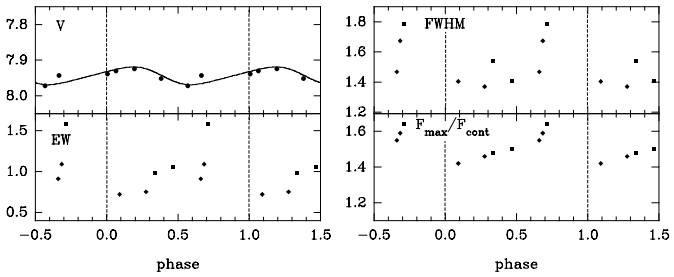

Fig. 6. a) *V* band light curve of *LQ Hya* in 1999 year and H_α line behavior as a function of rotational phase. Diamonds show the H_α data in 1998 December–1999 March, and squares show the H_α data in 1999 December.

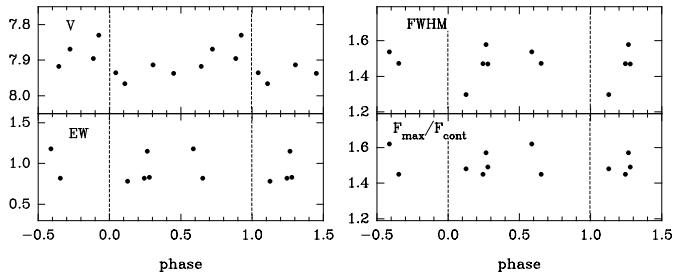

Fig. 6. b) *V* band light curve of *LQ Hya* in 2001 year and H_α behavior as a function of rotational phase.

chromosphere of *LQ Hya* radiates from 1 to 13% of the total stellar luminosity blocked by the starspots.

5. Conclusions

In this paper we present quasi-simultaneous photometric, polarimetric and spectroscopic data of surface inhomogeneities in the photosphere and the lower chromosphere of the young rapidly rotating dwarf *LQ Hya*. This study showed the following:

1. The photometric variability of *LQ Hya* can be described completely by the zonal starspots model. According to this model, the spot area of *LQ Hya* reaches up to 22% of the total stellar surface, and the temperature difference between the unspotted photosphere and the spots is about 800 K. These values agree with the results obtained by other authors using multicolor photometry, spectroscopy of TiO molecular bands and Doppler Imaging.
2. Starspots are localized on medium latitudes 24–48°. This conclusion agrees with results of Doppler Imaging showing the existence of medium latitude starspots, but does not confirm an existence of near-polar starspots shown by the same authors.
3. There is not a satisfactory agreement between the location of starspot pattern by our calculations (24–48° with the calculations of the flux tube rising in the assumption of both overshoot dynamo (30–70°) (Schüssler et al. 1996; Granzer et al. 2000) and distributed dynamo (near 50°) (Kitchatinov et al. 2000). On the other hand, there is no agreement with the fact that Doppler Imaging shows near-polar spots.
4. A comparison of our estimations of the mean starspot latitudes $< \phi >= \phi_0 + \Delta\phi/2$ with stellar photometric periods $P_{\rm phot}$ shows the growth of $P_{\rm phot}$ with increasing $< \phi >$. This effect indicates the stellar differential rotation with parameter $D_{\rm r} = 0.10$ (for the solar rotation parameter $D_{\rm r}$ is equal 0.19).
5. For the first time the broad-band linear polarization on *LQ Hya* was detected in all *UBVRI* bands. Its variability is caused by rotational modulation due to magnetic regions on the stellar surface with a filling factor of about 17−20% of the total stellar surface. This value agrees with the dark spot total area estimation obtained for the same year. This filling factor value may be underestimated.

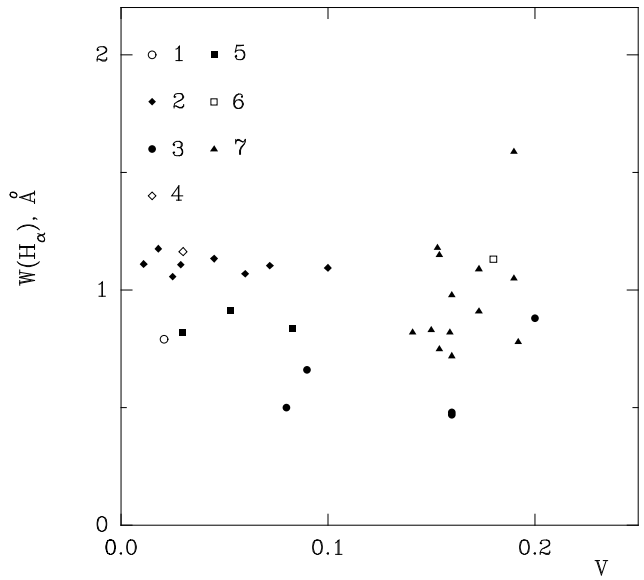

Fig. 7. a) The H_α pure emission equivalent width as a function of the stellar brightness. The symbols denotes data by different authors: 1: Fekel et al. (1986a,b); 2) Strassmeier et al. (1993); 3) Vilhu et al. (1991); 4) Montes et al. (1999); 5) Strassmeier et al. (1990); 6) Thatcher & Robinson (1993); 7) this paper.

6. The quasi-simultaneous photometric and spectroscopic observations in 1999 show a presence of chromospherically active regions (plages) which are concentrated near the most spotted longitudes. On the other hand, in 2001 the H_α emission parameters do not correlate with the starspots, indicating the uniformly longitudial distribution of plages or the primary contribution of a chromospheric network to the H_α emission in this year. An analysis of the H_α line shapes shows a combination of moving stellar plages and local velocity fields. Electron density estimations point to a "mixed" H_α line formation.
7. The estimation of plage area in the optically thick chromosphere may be realized in the framework of a black-body radiation model. For $T_{\rm chrom} = 10\,000$ K the H_α pure emission surface flux is about 3.4×10^7 erg c^{-1} cm^{-2} Å^{-1}. The H_α chromospheric luminosity of *LQ Hya* in 1999 and 2001 varied from 6.6×10^{28} to 1.3×10^{29}. Thus, the plage area of *LQ Hya* is about of 14% of the total surface, and is comparable with the spotarea.
8. A comparison of the spot area with the long-term H_α variations does not show any correlation. The bolometric luminosity deficit due to starspots is from 1.02×10^{31} to

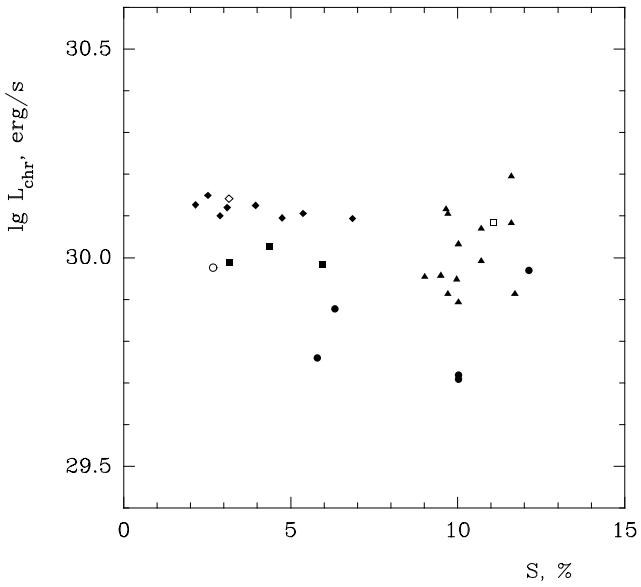

Fig. 7. b) The chromospheric emission on *LQ Hya* as a function of the spot area.

5.78×10^{31} erg/s. The stellar chromosphere radiates about 10% of the total energy blocked by starspots.

Acknowledgements. We want to thank Drs. K. G. Strassmeier and G. Cutispoto for having provided us with photometric and spectroscopic data for *LQ Hya*. We are grateful to Dr. K. G. Strassmeier for the *LQ Hya* Doppler maps. This work has been partially supported by Ukrainian SFFD grant No. 02.07/00300. We thank the referee M. Weber for constructive comments.

References

Alekseev, I. Yu. 1998, IV EAAS Meet. Proc. Moskow, 110
Alekseev, I. Yu. 1999, Bull. Crim. Ap. Observ., 95, 83
Alekseev, I. Yu. 2000, Astron. Rep., 44, 696
Alekseev, I. Yu. 2001, Low masses spotted stars. Astroprint, Odessa
Alekseev, I. Yu., & Bondar', N. I. 1998, Astron. Rep., 42, 655
Alekseev, I. Yu., & Gershberg, R. E. 1996a, Astron. Rep., 40, 538
Alekseev, I. Yu., & Gershberg, R. E. 1996b, Astron. Rep., 40, 528
Alekseev, I. Yu., & Gershberg, R. E. 1997, Astron. Rep., 41, 207
Alekseev, I. Yu., & Kozlova, O. V. 2000, Afz, 43, 339
Alekseev, I. Yu., & Kozlova, O. V. 2001, Afz, 44, 529
Alekseev, I. Yu., Gershberg, R. E., Katsova, M. M., & Livshits, M. A. 2001, Astron. Rep., 45, 482
Berdyugina, S. V., Ilyin, I. V., & Tuominen, I. 2001, in Cool Stars, Stellar Systems and the Sun, ed. R. J. Garcia López, R. Rebolo, & M. R. Zapatero Osorio, ASPCS, 223, 1207
Bessel, M. S. 1979, PASP, 91, 589
Boyd, L. J., Genet, R. M., Hall, D. S., et al. 1990, IAPPPC, 42, 44
Cram, L. E., & Mullan, D. J. 1979, ApJ, 234, 579
Cutispoto, G. 1991, A&AS, 89, 435
Cutispoto, G. 1993, A&AS, 102, 655
Cutispoto, G. 1996, A&AS, 119, 281
Cutispoto, G. 1998a, A&AS, 127, 207
Cutispoto, G. 1998b, A&AS, 131, 321
Cutispoto, G., Rodonó, M., & Messina, S. 2001, A&A, 367, 910
Donati, J.-F. 1999, MNRAS, 302, 457
Dorren, J. D. 1987, ApJ, 320, 756
Eaton, J. A., Henry, G. W., & Fekel, F. C. 1996, ApJ, 462, 888
Eggen, O. J. 1984, AJ, 89, 1358
Fekel, F. C, Bopp, B. W., Africano, J. L., et al. 1986a, AJ, 92, 1150
Fekel, F. C., Moffett, T. J., & Henry, G. W. 1986b, ApJS, 60, 551
Granzer, Th., Schüssler, M., Caligari, P., & Strassmeier, K. G. 2000, A&A, 335, 1087
Huovelin, Ju., & Saar, S. H. 1991, ApJ, 374, 319
Huovelin, Ju., Linnaluoto, S., Piirola, V., et al. 1985, A&A, 152, 357
Huovelin, Ju., Saar, S. H., & Tuominen, I. 1988, ApJ, 329, 882
Huovelin, Ju., Linnaluoto, S., Tuominen, I., et al. 1989, A&AS, 78, 129
Jetsu, L. 1993, A&A, 276, 345
Johnson, H. L. 1966, Ann. Rev. A&A, 4, 193
Kalmin, S. Yu. 1995, Kinemat. Phys. Cel. Bod. 11(3), 82
Kalmin, S. Yu., & Shakhovskoy, D. N. 1995, Kinemat. Phys. Cel. Bod. 11(3), 85
Kitchatinov, L. L., Jardine, M., & Donati, J.-F. 2000, MNRAS, 318, 1171
Montes, D., Saar, S. H., Collier Cameron, A., & Unruh, Y. C. 1999, MNRAS, 305, 45
Oláh, K., Kolláth, Z., & Strassmeier, K. G. 2000, A&A, 356, 643
Pettersen, B. R. 1987, Vistas Astron., 3, 41
Piirola, V. 1977, A&AS, 30, 213
Piirola, V. 1984, Observ. Astrophys. Lab. Univ. Helsinki. Rep., 6, 151
Piirola, V. 1988, in Polarized radiation of circumstellar origin, ed. G. V. Coyne, A. M. Magalhaes, A. F. J. Moffat, et al. (Vatican observatory), 735
Piskunov, N. E. 1992, in Stellar Magnetysm, ed. Yu. V. Glagolevskij, & I. I. Romanjuk (Nauka, St. Petersburg: Nauka), 92
Piskunov, N. E., Kupka, F., Ryabchikova, T. A., et al. 1995, A&AS, 112, 525
Piskunov, N. E., Kupka, F., Ryabchikova, T. A., et al. 1999, A&AS, 138, 119
Rice, J. B., & Strassmeier, K. G. 1998, A&A, 336, 972
Saar, S. H. 1996, in Stellar Surface Structure, ed. K. G. Strassmeier, & J. L. Linsky (Kluwer, Dordrecht), 237
Saar, S. H., & Huovelin, Ju. 1993, ApJ, 404, 739
Saar, S. H., & Neff, J. E. 1990, in Cool Stars, Stellar Systems and the Sun., ed. G. Wallerstein, ASPCS, 9, 171
Saar, S. H., Piskunov, N. E., & Tuominen, I. 1992, in Cool Stars, Stellar Systems and the Sun, ed. M. S. Giampapa, & J. A. Bookbinder, ASPCS, 26, 255
Saar, S. H., Piskunov, N. E., & Tuominen, I. 1994, in Cool Stars, Stellar Systems and the Sun, ed. J. P. Caillault, ASPCS, 64, 661
Schüssler, M., Caligari, P., Ferriz-Mas, A., et al. 1996, A&A, 314, 503
Shakhovskaya, N. I. 1974, Izv. Krim. Astrofiz. Obs., 51, 92
Strassmeier, K. G., & Hall, D. S. 1988, ApJS, 67, 453
Strassmeier, K. G., Fekel, F. C., Bopp, B. W., et al. 1990, ApJS, 72, 191
Strassmeier, K. G., Rice, J. B., Wehlau, W. H., et al. 1993, A&A, 268, 671
Strassmeier, K. G., Bartus, J., Cutispoto, G., & Rodonó, M. 1997, A&AS, 125, 11
Strassmeier, K. G., Serkowitsch, E., & Granzer, Th. 1999, A&AS, 140, 29
Sundland, S. R., Pettersen, B. R., Hawley, S. L., et al. 1988, in Activity in Cool Star Envelopes, ed. O. Havnes, B. R. Pettersen, J. H. M. M. Schmitt, & J. F. Solheim, (Kluwer, Dordrecht), 61
Thatcher, J. D., & Robinson, R. D. 1993, MNRAS, 262, 1
Unruh, Y. C. 1996, in Stellar Surface Structure, ed. K. G. Strassmeier, & J. L. Linsky (Kluwer, Dordrecht), 35
Van Hamme, W. 1993, AJ, 106, 2096
Vilhu, O., Gustafsson, B., & Walter, F. M. 1991, A&A, 241, 167